Estimation of Healthy and Fibrotic Tissue Distributions in DE-CMR Incorporating CINE-CMR in an EM Algorithm

Susana Merino-Caviedes[1], Lucilio Cordero-Grande[2], M. Teresa Sevilla-Ruiz[3],
Ana Revilla-Orodea[3], M. Teresa Pérez Rodríguez[4], César Palencia de Lara[4],
Marcos Martín-Fernández[1], and Carlos Alberola-López[1]

[1] Laboratorio de Procesado de Imagen, Universidad de Valladolid, Valladolid, Spain*
[2] Department of Biomedical Engineering, King's College London, London, UK
[3] Unidad de Imagen Cardiaca, Hospital Clínico Universitario de Valladolid, CIBER de enfermedades cardiovasculares (CIBERCV)
[4] Dpto. de Matemática Aplicada, Universidad de Valladolid, Valladolid, Spain

Abstract. Delayed Enhancement (DE) Cardiac Magnetic Resonance (CMR) allows practitioners to identify fibrosis in the myocardium. It is of importance in the differential diagnosis and therapy selection in Hypertrophic Cardiomyopathy (HCM). However, most clinical semiautomatic scar quantification methods present high intra- and interobserver variability in the case of HCM. Automatic methods relying on mixture model estimation of the myocardial intensity distribution are also subject to variability due to inaccuracies of the myocardial mask. In this paper, the CINE-CMR image information is incorporated to the estimation of the DE-CMR tissue distributions, without assuming perfect alignment between the two modalities nor the same label partitions in them. For this purpose, we propose an expectation maximization algorithm that estimates the DE-CMR distribution parameters, as well as the conditional probabilities of the DE-CMR labels with respect to the labels of CINE-CMR, with the latter being an input of the algorithm. Our results show that, compared to applying the EM using only the DE-CMR data, the proposed algorithm is more accurate in estimating the myocardial tissue parameters and obtains higher likelihood of the fibrosis voxels, as well as a higher Dice coefficient of the subsequent segmentations.

Key words: Scar segmentation · EM algorithm · Hypertrophic cardiomyopathy.

1 Introduction

Hypertrophic Cardiomyopathy (HCM) is the most prevalent cardiomyopathy of non-ischemic origin, with mortality rates between 1% and 5% [1]. One of

the clinical indicators in HCM is the volume of fibrosis in the myocardium. It may be measured using Delayed Enhancement (DE) Cardiac Magnetic Resonance (CMR), where fibrosis appears hyperenhanced with respect to myocardial healthy tissue. Current clinical segmentation methods for DE-CMR employ a prior mask of the myocardium, either obtained from CINE-CMR and aligned to DE-CMR if needed, or manually delineated on the image. A small remote myocardium region of interest (ROI) is also chosen to compute a threshold above which a voxel is considered fibrosis. However, the presence of diffuse fibrosis complicates selecting a threshold in HCM. In [2], it was observed that both inter- and intraobserver variability of manual and semiautomatic clinical methods were significantly higher in HCM than in either acute or chronic infarction.

Several proposed automatic scar segmentation methods are based on estimating the probability distribution of the healthy and scarred tissue [3,4] with the expectation maximization (EM) algorithm [5]. This approach is better suited to the use of more complex segmentation methods for identifying the scar, but misalignments in the myocardial prior mask may alter the estimated distributions. Moreover, the fibrosis distribution may be similar to the blood distribution. In [6], a multivariate mixture model to segment the myocardial contours in DE-CMR including CINE-CMR as well as T2-weighted images was proposed, where complementary modalities were used to solve ambiguities in borders. However, this method uses the same label partition for all the modalities and relies on an atlas for its initialization. Therefore, its adaptation to fibrosis segmentation in HCM is not straightforward.

Here, the variability of the tissue distribution estimations with respect to displacements in the prior myocardial mask is explored. We propose an EM algorithm for the estimation of all tissue distributions in DE-CMR using CINE-CMR and a prior myocardial mask. In the proposed algorithm, the label partitions of DE-CMR and CINE-CMR do not need to be the same. Additionally, small misalignments between both modalities are considered. The experimental results show that the proposed EM parameter estimations have lower error with respect to the classic EM algorithm on the DE-CMR myocardial mask. The scar segmentations obtained by applying the maximum likelihood (ML) criterion with the parameters estimated by the proposed method achieved a higher Dice coefficient than the classic EM method as well.

The rest of the document is structured as follows: in Section 2, the proposed EM method is described, followed by Section 3, where the experimental setup and results are shown. Finally, some conclusions are drawn in Section 4.

2 Methods

Let $I_C(\mathbf{x}, t) : \Omega \times [0, T] \to \mathbb{R}$ be a spatiotemporal CINE-CMR image, where T is the cardiac cycle period and $\Omega \subset \mathbb{R}^D$ is the image spatial domain. Let $I_R(\mathbf{x})$ be a DE-CMR image acquired at an instant $t = t_R \in [0, T]$. We define the label sets $\mathcal{L} = \{L_i\}_{i=1}^{N_L} = \{C, H, S, B\}$ for DE-CMR and $\mathcal{A} = \{A_i\}_{i=1}^{N_A} = \{C, M, B\}$ for CINE-CMR, where $N_L = 4$, $N_A = 3$, and the labels C, M, H, S and B stand

respectively for the blood cavity enclosed by the endocardium, the myocardium, the healthy tissue, the scar and the background. Finally, let $\widehat{A}(\mathbf{x}) : \Omega \to \mathcal{A}$ be an anatomical segmentation that assigns to $\mathbf{x}$ its estimated CINE-CMR label at time t_R.

The Rice distribution is employed to model a single tissue intensity distribution in magnetic resonance imaging. The Rayleigh and the Gaussian distributions, appropriate particular cases of the general Rice distribution, have been used to model the healthy tissue and the blood intensity distributions, respectively [3,4]. The intensity distribution of each particular tissue in DE-CMR is assumed to have invariant parameters with respect to the CINE-CMR intensity $I_C(\mathbf{x}, t_R)$ (from now on, $I_C(\mathbf{x}, t_R) = I_C(\mathbf{x})$ for clarity) and anatomical segmentation $\widehat{A}(\mathbf{x})$; that is, if $L_i(\mathbf{x})$ is known for a given pixel $\mathbf{x}$, then $P(I_R(\mathbf{x})|I_C(\mathbf{x}), L_i(\mathbf{x}), A_k(\mathbf{x})) = P(I_R(\mathbf{x})|L_i(\mathbf{x}))$. However, both the labels L_i and the distribution parameters for each L_i are unknown. For this reason, it seems reasonable to use the Expectation Maximization (EM) algorithm [5] to estimate these parameters. Let $\bar{\theta}$ be the parameters required in order to characterize all DE-CMR tissue distributions. The image loglikelihood is:

$$
\begin{aligned}
\log L(\bar{\theta}) &= \sum_{\mathbf{x}_n \in \Omega} \log \sum_{j=1}^{N_L} P(I_R(\mathbf{x}_n), I_C(\mathbf{x}_n), L_j; \bar{\theta}) \\
&= \sum_{\mathbf{x}_n \in \Omega} \log \sum_{j=1}^{N_L} \sum_{k=1}^{N_A} P(I_R(\mathbf{x}_n), I_C(\mathbf{x}_n), L_j, A_k; \bar{\theta})
\end{aligned}
\tag{1}
$$

where the second identity comes from applying the law of total probability using the CINE-CMR labels. In order to estimate the $\bar{\theta}$ that maximizes the log likelihood, we modify the EM method so that it takes into account the CINE-CMR label probabilities. Therefore, let $Q_{jk}(\mathbf{x})$ be such that $Q_{jk}(\mathbf{x}) \geq 0$ and $\sum_{j=1}^{N_L} \sum_{k=1}^{N_A} Q_{jk}(\mathbf{x}) = 1$. Then:

$$
\begin{aligned}
\log L(\bar{\theta}) &= \sum_{\mathbf{x}_n \in \Omega} \log \sum_{j=1}^{N_L} \sum_{k=1}^{N_A} P(I_R(\mathbf{x}_n), I_C(\mathbf{x}_n), L_j, A_k; \bar{\theta}) \\
&= \sum_{\mathbf{x}_n \in \Omega} \log \sum_{j=1}^{N_L} \sum_{k=1}^{N_A} Q_{jk}(\mathbf{x}_n) \frac{P(I_R(\mathbf{x}_n), I_C(\mathbf{x}_n), L_j, A_k; \bar{\theta})}{Q_{jk}(\mathbf{x}_n)} \\
&\geq \sum_{\mathbf{x}_n \in \Omega} \sum_{j=1}^{N_L} \sum_{k=1}^{N_A} Q_{jk}(\mathbf{x}_n) \log \frac{P(I_R(\mathbf{x}_n), I_C(\mathbf{x}_n), L_j, A_k; \bar{\theta})}{Q_{jk}(\mathbf{x}_n)} = J(\bar{\theta})
\end{aligned}
\tag{2}
$$

by the application of Jensen's inequality[5]. The joint probabilities may be expressed as (dropping the $\mathbf{x}_n$ dependence for clarity):

$$
P(I_R, I_C, L_j, A_k; \bar{\theta}) = P(I_R|I_C, L_j, A_k; \bar{\theta})P(L_j|I_C, A_k)P(I_C|A_k)P(A_k) \tag{3}
$$

---

[5] Jensen's inequality states that if f is a concave function and X is a random variable, then $E[f(X)] \leq f(E[X])$.

The $P(I_C(\mathbf{x}_n)|A_k), k = 1, 2, 3$ are estimated from $\widehat{A}(\mathbf{x})$ and the CINE-CMR intensity distributions as smoothed normalized histograms. Regarding $P(A_k)$, it is modeled so that the probability decays when the distance to the considered CINE-CMR ROI increases. Its computation uses a Gaussian filter $g(\mathbf{x}, \sigma)$ with $\sigma = d/3$, where d is a parameter for the maximum distance the myocardial contours are expected to be misaligned. Then, $P(A_k) = (\chi(\widehat{A}(\mathbf{x}), A_k) * g(x, d/3))/(\sum_{l=1}^{N_A} \chi(\widehat{A}(\mathbf{x}), A_l) * g(x, d/3))$, where $\chi(z, A_l) = 1$ if $z = A_l$ and 0 otherwise. Since $P(L_j|A_k)$ are also unknown, the method should also provide their estimates, which will be referred to as π_{jk}. Since they are conditional probabilities, they obey $\pi_{jk} \geq 0$ and $\sum_{j=1}^{N_L} \pi_{jk} = 1$. $Q_{jk}(\mathbf{x})$ is chosen so that $J(\bar{\theta})$ is as close as possible to $\log L(\bar{\theta})$, and it takes the expression:

$$Q_{jk}(\mathbf{x}_n) = \frac{P(I_R(\mathbf{x}_n), L_j, A_k; \bar{\theta})}{\sum_{\hat{j}=1}^{N_L} \sum_{\hat{k}=1}^{N_A} P(I_R(\mathbf{x}_n), L_{\hat{j}}, A_{\hat{k}}; \bar{\theta})} = P(L_j, A_k|I_R(\mathbf{x}_n); \bar{\theta}) \quad (4)$$

Regarding the maximization step, a new value for $\bar{\theta}$ is chosen as the argument that maximizes $J(\bar{\theta})$, considering $Q_{ij}(\mathbf{x}_n)$ as fixed.

$$\widehat{\bar{\theta}}, \widehat{\bar{\pi}} = \arg \max_{\bar{\theta}, \bar{\pi}} J(\bar{\theta})$$

$$= \arg \max_{\bar{\theta}, \bar{\pi}} \sum_{\mathbf{x}_n \in \Omega} \sum_{j=1}^{N_L} \sum_{k=1}^{N_A} Q_{jk}(\mathbf{x}_n)\big(\log P(I_R(\mathbf{x}_n)|L_j, A_k; \bar{\theta}) + \log \pi_{jk} \quad (5)$$

$$+ \log P(A_k) - \log Q_{jk}(\mathbf{x}_n)\big)$$

In order to estimate $\widehat{\bar{\theta}}$, the first derivatives are set to zero. Given the assumption $P(I_R(\mathbf{x}_n), L_j, A_k; \bar{\theta}) = P(I_R(\mathbf{x}_n), L_j; \bar{\theta})$, problem (5) is equivalent to:

$$\widehat{\bar{\theta}} = \arg \max_{\bar{\theta}} \sum_{\mathbf{x}_n \in \Omega} \sum_{j=1}^{N_L} \log P(I_R(\mathbf{x}_n)|L_j; \bar{\theta}) \sum_{k=1}^{N_A} Q_{jk}(\mathbf{x}_n) \quad (6)$$

For the computation of $\widehat{\bar{\pi}}$, the method of the Lagrange multipliers is employed, so that the augmented problem is:

$$\widehat{\pi_{jk}} = \arg \max_{\pi_{ml}} \sum_{\mathbf{x}_n \in \Omega} \sum_{m=1}^{N_L} \sum_{l=1}^{N_A} Q_{ml}(\mathbf{x}_n) \log \pi_{ml} - \lambda(\sum_{m=1}^{N_L} \pi_{mk} - 1) \quad (7)$$

The solution of (7) has the following closed form:

$$\widehat{\pi_{jk}} = \frac{\sum_{\mathbf{x}_n \in \Omega} Q_{jk}(\mathbf{x}_n)}{\sum_{\mathbf{x}_n \in \Omega} \sum_{m=1}^{N_L} Q_{mk}(\mathbf{x}_n)} \quad (8)$$

Since the EM algorithm finds local maxima, the choice of initial values for the parameters greatly influences the output estimates. In our method, these initial parameters are computed using the CINE-CMR labels, sometimes combined with heuristics based on clinical criteria.

– The blood tissue is modeled by a Gaussian distribution whose parameters are estimated by the maximum likelihood (ML) criterion on the voxels labeled as cavity in CINE-CMR.

– The healthy myocardial tissue is modeled by a Rayleigh distribution. Its parameter is estimated from the mode of the histogram computed from the voxels labeled as myocardium in CINE-CMR [7].

– The scar intensity distribution is assumed to be close enough to a Gaussian. Its mean is initialized at 5 standard deviations over the mean of the estimated healthy myocardium, and its standard deviation is initialized to the same initial standard deviation of the healthy tissue distribution. This makes use of the findings in [8].

– The background is composed of a number of different tissues. For this reason, this distribution is not estimated as a parametric model, but as a normalized histogram, smoothed by a Gaussian kernel with a standard deviation of 0.8, of the voxels labeled as background.

– The π_{ij} are initialized as the (i,j)-th element of the matrix $\begin{pmatrix} 0.7 & 0.1 & 0.1 \\ 0.1 & 0.4 & 0.1 \\ 0.1 & 0.4 & 0.1 \\ 0.1 & 0.1 & 0.7 \end{pmatrix}$.

Table 1. Imaging parameters of the acquired CMR sequences.

Settings	SAx-C	SAx-LE	2C-C	4C-C
Acquisition sequence	sBTFE BH	PSIR_TFE BH	sBTFE BH	sBTFE BH
View	SAx	SAx	2C LAx	4C LAx
Temporal phases	30	1	30	30
FOV/Frequency Encoding Steps	1.98–2.01 mm	1.98–2.01 mm	1.98–2.00 mm	1.98–2.00 mm
In-plane pixel spacing	0.93–1 mm	0.55–0.62 mm	1.18–1.25 mm	0.81–1 mm
Slice thickness (gap)	10 (0) mm	10 (0) mm	8 (0) mm	8 (0) mm
Number of slices	9–13	9–12	1	3
Echo time	1.60–1.79	2.99	1.59–1.83	1.71–1.89
Repetition time	3.18–3.57	6.09–6.14	3.18–3.66	3.41–3.79
Flip Angle	45	25	45	45

BH: Breath Hold. FOV: Field of View.

3   Experimental Results

For this work, 21 patients with hypertrophic cardiomyopathy (HCM) underwent a cardiac MRI study, each of which contained CINE sequences in short axis (SAx), two chamber (2C) and four chamber (4C) long axis (LAx), and a SAx DE-CMR sequence. All sequences were acquired with a 3T Philips Achieva MR scanner, and their main acquisition parameters are summarized in Table 1.
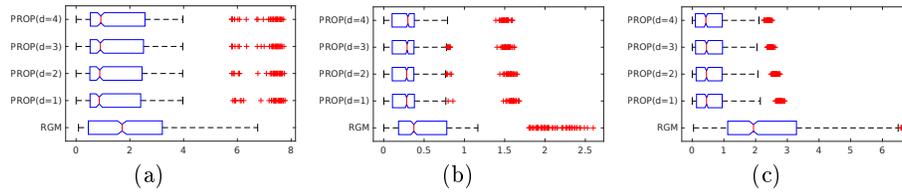
Fig. 1. Boxplots of the normalized absolute deviations of (a) the healthy tissue intensity mode, (b) the fibrosis mean and (c) the fibrosis standard deviation computed by the EM methods with respect to the respective ML estimates on ROI_r and ROI_s.

The epicardial and endocardial SAx-C contours at end-diastole were delineated by cardiologists. From them and SAx-C, the $P(I_C|A_k)$ distributions were estimated. In DE-CMR, the fibrosis ROI (ROI_s) was defined by a manually selected threshold, applied on a myocardial ROI (ROI_m) conservatively drawn to avoid including false positives after thresholding and scars of other pathologies. Additionally, a small ROI (ROI_r) of remote myocardium (healthy tissue far away from the septum) was drawn, and a voxel whose brightness was considered by the cardiologists as the maximum fibrosis brightness $I_R^{S,\max}$.

In order to simulate the variability in the myocardial contours of registration methods and to study the effect of false positives due to contour misalignments in the distributions estimation, a second set of myocardial masks were drawn on the SAx-LE images for each patient and 30 realizations of in-plane translations with random orientation uniformly distributed in the range $[0, 2\pi)$ and norm of 3 mm. were applied to the myocardial contours of each slice. The resulting masks were our test set of myocardial masks. The SAx-C and SAx-LE volumes were spatially aligned using the framework described in [9], which also corrects breath hold misalignments. The SAx-C volume at t_R was transformed to the SAx-LE space and resolution.

For all patients and the test set of myocardial masks, a Rayleigh-Gaussian mixture (RGM) was estimated on the myocardium, and the proposed EM algorithm (PROP) was run with an expected maximum distance to misalignments $d = 1, 2, 3, 4$. Additionally, the intensity distribution parameters of ROI_s and ROI_r were estimated on each patient by the ML criterion. The absolute deviation of the EM estimated parameters with respect to the parameters estimated on ROI_s and ROI_r, normalized by the latter, are visualized as boxplots in Fig. 1. It may be observed that the proposed method provides parameters more similar to the ones computed on ROI_s and ROI_r. In addition, the estimations present less error variance with respect to the RGM method, and similar results for every d employed.

The mean loglikelihood (mLL) yielded by the estimated parameters was computed on ROI_s and ROI_r. Their mean and standard deviation are given in Table 2. For each experiment, a fibrosis mask was generated as the voxels contained in ROI_m where $P(L_S|I_R(\mathbf{x}), \bar{\theta}) > P(L_H|I_R(\mathbf{x}), \bar{\theta})$. This mask was compared with the ROI_s by means of the Dice coefficient. Their means and standard de-

Table 2. Mean loglikelihood (mLL) on ROI_s and ROI_r, and Dice coefficient of the ensuing segmentations. Measures are given as mean $\pm$ standard deviation.

Method	Extra Inputs	mLL in ROI_r	mLL in ROI_s	Dice coefficient
RGM	—	-5.551 $\pm$ 0.851	-4.287 $\pm$ 0.671	0.473 $\pm$ 0.304
PROP(d=1)	—	-5.603 $\pm$ 1.270	-4.254 $\pm$ 1.472	0.541 $\pm$ 0.254
PROP(d=2)	—	-5.597 $\pm$ 1.244	-4.220 $\pm$ 1.402	0.545 $\pm$ 0.257
PROP(d=3)	—	-5.602 $\pm$ 1.229	-4.198 $\pm$ 1.328	0.543 $\pm$ 0.258
PROP(d=4)	—	-5.615 $\pm$ 1.235	-4.218 $\pm$ 1.302	0.537 $\pm$ 0.261
5SD	ROI_r	—	—	0.482 $\pm$ 0.254
FWHM	$ROI_r, I_R^{S,\max}$	—	—	0.589 $\pm$ 0.287

viations are also included in Table 2. Figure 2 shows an example of the averaged segmentations with the test myocardial set with RGM and PROP($d = 3$).

It may be observed that the proposed method achieved higher mean mLL in the fibrosis ROI, but lower mean mLL in the remote myocardium ROI. With respect to the Dice coefficient, the proposed method achieved higher Dice mean values, as well as lower standard deviations than the RGM method. Kruskal-Wallis tests at a 1% significance level on the mLL of each ROI and the Dice coefficient rejected the null hypothesis of having the same median for the mLL of fibrosis and the Dice coefficient with $p < 10^{-12}$ and $p < 10^{-5}$ respectively, and accepted it for the mLL of healthy tissue with $p = 0.81$. Conducting paired Mann-Whitney U tests at 5% significance level between the RGM and the PROP method with all d values indicated that the median Dice coefficient with the PROP method was higher than the median Dice coefficient with the RGM, with $p < 10^{-9}$ in all tests. From these values it may be inferred that the proposed EM method is better at identifying fibrosis than the classic RGM EM method in the presence of false positives introduced by myocardial contour delineation errors, even if the mLL of healthy tissue is slightly decreased. In Table 2, the Dice coefficient results of two methods used in clinical practice, which require additional user interaction, are also given. The 5 standard deviations over the remote myocardium mean method (5SD) behaves slightly better than the RGM, but yields lower Dice coefficient values than the PROP method. The Full Width at Half Maximum (FWHM) method achieves the best results, at the expense of requiring the cardiologist to delineate ROI_r and selecting a fibrosis voxel with maximum DE-CMR intensity $I_R^{S,\max}$, which the proposed method does not need.

4 Conclusions

In this work, an EM algorithm that takes into account the information of two images from different cardiac CMR modalities (DE-CMR and CINE-CMR) has been proposed. This algorithm is designed so that the number of labels on each modality do not need to be the same, and without assuming perfect alignment between modalities. Compared to the Rayleigh-Gaussian mixture model often
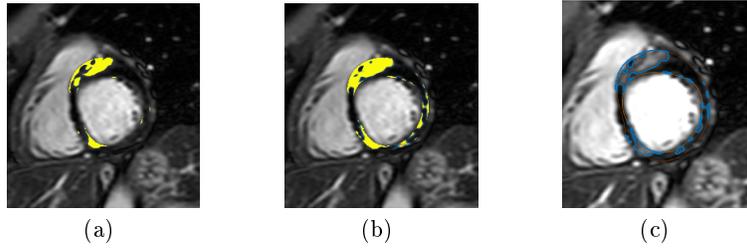
(a)   (b)   (c)

Fig. 2. SAx-LE slice with overlapped mean outcome of the ML segmentation using (a) the RGM method and (a) the PROP method. (c) Manual delineations.

used in the literature, the proposed method achieved lower normalized absolute deviations in the parameter estimates, as well as improved Dice coefficient of the segmentations performed by the ML criterion. Our future work includes studying the partial volume effect influence on the algorithm.

References

1. Bruder, O., Wagner, A., Jensen, C.J., Schneider, S., Ong, P., Kispert, E.M., Nassenstein, K., Schlosser, T., Sabin, G.V., Sechtem, U., Mahrholdt, H.: Myocardial scar visualized by cardiovascular magnetic resonance imaging predicts major adverse events in patients with hypertrophic cardiomyopathy. J Am Coll Cardiol **56**(11) (2010) 875–887
2. Flett, A.S., Hasleton, J., Cook, C., Hausenloy, D., Quarta, G., Ariti, C., Muthurangu, V., Moon, J.C.: Evaluation of techniques for the quantification of myocardial scar of differing etiology using cardiac magnetic resonance. JACC: Cardiovas Imaging **4**(2) (2011) 150–156
3. Hennemuth, A., Seeger, A., Friman, O., Miller, S., Klumpp, B., Oeltze, S., Peitgen, H.O.: A Comprehensive Approach to the Analysis of Contrast Enhanced Cardiac MR Images. IEEE Trans Med Imaging **27**(11) (2008) 1592–1610
4. Elagouni, K., Ciofolo-Veit, C., Mory, B.: Automatic segmentation of pathological tissues in cardiac mri. In: IEEE Int Symp Biomed Imaging, Rotterdam, Netherlands (April 2010) 472–475
5. Dempster, A.P., Laird, N.M., Rubin, D.B.: Maximum likelihood from incomplete data via the EM algorithm. J R Stat Soc Series B (Methodol) **39**(1) (1977) 1–38
6. Zhuang, X., Shen, J.: Multi-scale patch and multi-modality atlases for whole heart segmentation of MRI. Med Image Anal **31** (2016) 77–87
7. Aja-Fernández, S., Tristán-Vega, A., Alberola-López, C.: Noise estimation in single- and multiple-coil magnetic resonance data based on statistical models. Magn Reson Imaging **27**(10) (2009) 1397–1409
8. Aquaro, G., Positano, V., Pingitore, A., Strata, E., Di Bella, G., Formisano, F., Spirito, P., Lombardi, M.: Quantitative analysis of late gadolinium enhancement in hypertrophic cardiomyopathy. J Cardiov Magn Reson **12**(1) (2010) –
9. Cordero-Grande, L., Merino-Caviedes, S., Alba, X., Figueras i Ventura, R.M., Frangi, A.F., Alberola-Lopez, C.: 3D fusion of cine and late-enhanced cardiac magnetic resonance images. In: 9th IEEE Int Symp Biomed Imaging, Barcelona, Spain (2012) 286–289